Reference: *Biol. Bull.* **197:** 82–93. (August 1999)

# Morphology and Epithelial Ion Transport of the Alkaline Gland in the Atlantic Stingray (*Dasyatis sabina*)

GREGORY M. GRABOWSKI,[1] JOHN G. BLACKBURN,[2] AND ERIC R. LACY[3,4]

[1] *Department of Biology, University of Detroit Mercy, 4001 W. McNichols, P.O. Box 19900, Detroit, Michigan 48219;* [2] *Department of Physiology,* [3] *Department of Cell Biology and Anatomy, Medical University of South Carolina, 171 Ashley Avenue, Charleston, South Carolina 29425; and* [4] *Marine Biomedicine and Environmental Sciences, Medical University of South Carolina, 221 Fort Johnson Road, Charleston, South Carolina 29412*

**Abstract.** The alkaline glands are two fluid-filled sacs that lie on the ventral, posterior surface of each kidney in skates and rays. In this study, the morphology, transepithelial ion transport, fluid constituents, and histochemistry of the alkaline glands of the Atlantic stingray, *Dasyatis sabina*, were investigated. The duct from each gland joined the corresponding vas deferens and the resulting two common ducts emptied into the cloaca. Dark burgundy, aqueous fluid (pH 8.0–8.2) was secreted into the sacs by a simple columnar epithelium with extensive rough endoplasmic reticulum and large secondary lysosomes containing lipofuscin and membrane fragments. Zonulae occludentes were deep (~22 fibrils), reflecting an electrically tight epithelium (732 ohms/cm$^2$). Carbonic anhydrase activity was localized histochemically within the intercellular spaces and less intensely in the mid-basal cytoplasm.

*In vitro* electrophysiology showed that baseline short-circuit current (Isc, 29.1 $\mu$A/cm$^2$) was reduced 67.0% after $Cl^-$ removal from the medium. $Cl^-$ removal also completely abolished luminal alkalinization (baseline 4.5 $\pm$ 0.7 $\mu$Eq of acid/cm$^2$/h). Luminal exposure to the chloride-bicarbonate exchange inhibitor, DIDS, reduced Isc by 38%. Simultaneous administration of DIDS and bumetanide ($Na^+/K^+/Cl^-$ cotransport inhibitor) to the serosal side of the tissue caused the Isc to decrease >100%. Serosal exposure to ouabain (Na-K, ATPase inhibitor) decreased Isc 48%, whereas amiloride (sodium ion channel blocker) and acetazolamide (carbonic anhydrase inhibitor) had no statistically significant effect on Isc or alkalinization rates. Taken together the results suggest the presence of apical epithelial bicarbonate exchangers that are chloride or sodium dependent, basal sodium and $HCO_3^-$ transport, and an Isc that is not totally dependent on $Na^+$-$K^+$ ATPase.

Received 12 April 1999; accepted 14 June 1999.

Send correspondence to Eric R. Lacy, Marine Biomedicine and Environmental Sciences, Medical University of South Carolina, 221 Fort Johnson Road, Charleston, SC 29412.

A portion of this work was presented in abstract form (The FASEB Journal, Part I, #3024, 1992).

## Introduction

Early anatomical studies of the male skate and stingray urogenital system reported a pair of blind-ended sacs, each of which opened into the cloaca. These structures were described initially as urinary bladders or sperm storage sacs (Borcea, 1906; Daniel, 1934), but the only evidence to support this functional nomenclature is the proximity of the sacs' openings to those of the ureters and vas deferens within the cloaca.

The sacs secrete and store a watery fluid of high pH (8.0–9.2), thus their name, alkaline gland (Maren *et al.*, 1963). On the basis of the high pH of the fluid, Smith (1929) speculated that it neutralized the potentially deleterious effects of acidic urine in the cloaca on the extruded sperm. As yet, however, no studies on the physiological function of the alkaline gland have been published.

A few reports, from various skate species (little skate, *Raja erinacea;* barndoor skate, *R. stabuliforis;* big skate, *R. ocellata*), have described the gland's morphology and epithelial transport physiology (H.W. Smith, 1929; Maren *et*

*al.,* 1963; Masur, 1984; P. L. Smith, 1981, 1985). These morphological accounts show that the gland lumen has mucosal "villar projections" lined by a simple columnar epithelium (Maren *et al.,* 1963; Masur, 1984). The mucosa generates and maintains a hundred-fold concentration gradient of OH ions and a 50-fold gradient of $CO_2$ from plasma to gland lumen; these are some of the steepest alkaline gradients across any epithelium in nature (Maren *et al.,* 1963). Given the unique epithelial transport properties of the alkaline gland, physiologic studies have focused on the mechanisms of fluid and bicarbonate secretion (Maren *et al.,* 1963; Smith, 1981, 1985).

Chloride and bicarbonate are the two main anions constituting alkaline gland fluid in the skate. *In vitro* experiments indicate that chloride secretion accounts for most, if not all, of the short-circuit current (Isc) (Maren *et al.,* 1963; Smith, 1981, 1985). These results led to speculation that chloride-dependent bicarbonate transport might be involved in fluid alkalinization. Although definitive evidence was lacking, secreted chloride was believed to recirculate into the epithelial cell by way of a $Cl^-/HCO_3^-$ exchanger located at the apical plasma membrane (Maren *et al.,* 1963; Smith, 1981, 1985). Carbonic anhydrase, an enzyme associated with many bicarbonate-secreting tissues, was identified biochemically in the alkaline gland of some but not all skate species studied (Maren *et al.,* 1963). The concentration of carbonic anhydrase in the tissue was correlated with the pH of the alkaline gland fluid produced (Maren *et al.,* 1963), suggesting that this enzyme has a role in bicarbonate secretion for some skate species.

The present study uses transmission and scanning electron microscopy and freeze fracture to elucidate the ultrastructural organization of the alkaline gland in a stingray species, *Dasyatis sabina,* the Atlantic stingray. The presence and distribution of carbonic anhydrase activity, nerve fibers, and lipofusion were identified histochemically. These results are correlated with *in vitro* electrophysiological data and rates of fluid alkalinization. Some of the regulatory mechanism of ion transport were probed with various metabolic inhibitors. The composition of the fluid removed from the alkaline glands was analyzed.

## Materials and Methods

Sexually mature male Atlantic stingrays (*Dasyatis sabina,* wing span ~45 cm) purchased from Gulf Specimens Inc. (Panacea, FL) or captured along the coast of South Carolina were allowed to acclimate in a 16,000-l holding tank for at least 5 days prior to experimentation. Water in the holding tank was drawn from Charleston (South Carolina) Harbor (650–850 mosm/l) and maintained at room temperature. Stingrays were fed shrimp twice a week and kept on a 12-h light/dark cycle. After acclimation, animals were anesthetized with MS222 (3-aminobenzoic acid ethyl ester, 0.5 g/l, Sigma Chemical Co.) and double pithed. The body cavity was opened by a ventral midline incision; the alkaline gland fluid was aspirated with a 25-gauge needle and saved at 4°C for further analysis; the alkaline gland was removed for use in morphology or electrophysiology experiments.

### *Light and electron microscopy*

Fixative (2.5% paraformaldehyde, 5.0% glutaraldehyde, and 0.25% picric acid; Ito and Karnovsky, 1968) was injected into both sacs of the gland immediately after the fluid was removed. After 1 h the puboischiac bar was severed, and the alkaline gland was freed from surrounding tissue with fine forceps. Each gland was excised at its junction with the cloacal wall and placed in the same fixative for 24 h. The tissue was then rinsed, trimmed into 1-$mm^2$ pieces with a razor blade, and stored in 0.1 *M* sodium cacodylate buffer.

Alkaline gland fluid was centrifuged at 200 × *g* for 10 min. The pellet was fixed for 4 h in the same fixative injected into the gland sacs (Ito and Karnovsky, 1968). Both pellet and pieces of fixed gland were then postfixed (1.0% osmium tetraoxide in 0.1 *M* sodium cacodylate buffer), dehydrated in graded ethanols, and embedded in Epon-Araldite. Sections were cut, stained (semithin sections stained with alkalinized toluidine blue and ultrathin sections with uranyl acetate and lead citrate), and examined using a light microscope or a JEOL 1200 EX electron microscope.

Additional gland tissue, fixed as described above but in aldehydes only, was cryoprotected in graded concentrations of glycerols to a final concentration of 30% glycerol for freeze fracture. The tissue was then frozen rapidly in liquid propane, followed by fracturing and replication in a Balzer 360 M device (Balzers, Fürstentum Liechtenstein). Replicas were supported on 200-mesh copper grids and examined with the transmission electron microscope.

Aldehyde-fixed tissue was also used for scanning electron microscopy. It was first postfixed in 1.0% osmium tetraoxide in 0.1 *M* sodium cacodylate buffer, followed by dehydration in graded ethanols, and then critical point dried using a Sorvall critical point dryer (Newtown, CT). Tissue was coated with gold/palladium for 3 min at 2.5 kV and 20 mA using an E5100 sputter coating unit (Polaron Instruments, Doylestown, PA) and examined with a JEOL 35C scanning electron microscope.

### *Lipofuscin staining*

Alkaline gland tissue and particulate matter from gland fluid of four stingrays were stained for lipofuscins using the Long Ziehl-Neelsen technique (Bancroft and Cook, 1984). The pellet, as described above, and gland tissue were fixed in Bouin's solution for 2 h, followed by dehydration in graded ethanols, clearing in xylene, and embedding in par-

affin. Five-micrometer-thick sections were deparaffinized in xylene taken stepwise to water and stained in filtered carbol fuchsin for 1–3 h at 56°C. After staining, sections were washed in water, differentiated in 1% acid-alcohol, and counter stained in aqueous methylene blue. Slides were then rinsed in water, dehydrated, cleared in xylene, and mounted on glass slides. Lipofuscin appeared bright magenta, and nuclei stained blue against a pale magenta background.

*Silver staining of neural tissue*

Nerve fibers in alkaline glands were localized using the silver precipitate method of Sevier and Munger (1965). Five-micrometer-thick paraffin sections of Bouin's fixed tissue were incubated in 20% silver nitrate for 15 min, washed with distilled water, and developed in ammoniacal silver (10% silver nitrate precipitated with 28%–30% ammonium hydroxide, plus 2% formalin). After a 2-min rinse in 5% sodium thiosulfate, slides were washed in distilled water, dehydrated, cleared in xylene, and mounted.

*Localization of carbonic anhydrase activity (CAH)*

Alkaline glands were fixed in a solution of 2.0% paraformaldehyde, 2.5% glutaraldehyde, and 0.4% $CaCl_2$ in 0.1 *M* sodium cacodylate buffer for localization of carbonic anhydrase activity (CAH) using the Hansson's technique (Hansson, 1967; Maren, 1980b; Sugai and Ito, 1980; Lacy, 1983b). Fixed tissue was frozen in 8% sucrose and sectioned at 10 $\mu$m on an IEC CTF cryostat (International Equipment Company). Sections were floated on Hansson's medium (1.86 m*M* $CoSO_4$, 55.9 m*M* $H_2SO_4$, 3.73 m*M* $KH_2PO_4$, and 158 m*M* $NaHCO_3$) for 1–5 min. Sections were rinsed by floating on Sorensen's phosphate buffer (pH 8.0) for 1 min and then transferred onto 2% ammonium sulfide for 1–2 min. This was followed by rinsing sections on Sorensen's phosphate buffer at pH 5.0 and then mounting them in heated glycerin jelly on glass slides for observation with a light microscope (Sugai and Ito, 1980; Lacy, 1983b). After the sections were incubated on 2% ammonium sulfide, low-pH buffers were used to prevent the black precipitate indicative of CAH activity from degrading. For electron microscopy, sections were postfixed in 1.0% osmium tetraoxide in Sorensen's phosphate buffer (pH 5.0) for 30–45 min, stained *en bloc* with 1.0% uranyl acetate in maleate buffer (pH 5.2), dehydrated in graded ethanols, and embedded flat in epoxy resin. Ultrathin sections were stained and examined as described above.

Acetazolamide ($10^{-5}$ and $10^{-6}$ *M*) in Hansson's medium was used to inhibit CAH, thereby serving as a negative control. For evaluation of nonspecific activity, sections were incubated either in ammonium sulfide without prior incubation on Hansson's medium, or on bicarbonate-free Hansson's medium.

*Morphometric analysis*

Ratios of basal cells to columnar cells were determined from counts made of cross-sectioned glands at the light microscopic level (epoxy resin sections, 50×). The size and distribution of intramembranous particles observed in freeze fracture replicas were measured on electron micrographs using a scale magnification loupe (Baxter, Atlanta, GA). The luminal surface area of columnar epithelial cells was estimated by measuring the cell diameters of luminal plasma membranes from scanning electron micrographs.

*Constituents of alkaline gland fluid*

Fluid from the alkaline glands of five stingrays was pooled, cooled to 5°C, and centrifuged as described above. The supernatant was then frozen by placing the tube in dry ice and shipped overnight to Mayo Medical Laboratories (Rochester, MN) for analysis of its composition.

*Electrophysiology*

Each sac of the alkaline gland was freed *in situ* from surrounding connective tissue, excised, and placed in a petri dish of oxygenated elasmobranch Ringer (NaCl, 280.0 m*M*; KCl, 5.0 m*M*; $MgCl_2$, 3.3 m*M*; $CaCl_2$, 3.8 m*M*; $NaHCO_3$, 10.0 m*M*; urea, 350.0 m*M*; dextrose, 5.0 m*M*; 800 mOsm/l; pH 6.9). The Ringer was gassed with 95% $O_2$/5% $CO_2$, unless otherwise noted, and used at room temperature.

Each sac was mounted between two halves of an Ussing chamber (4-mm diameter). Each half of the chamber was connected to a 20-ml circulation reservoir (Medical Research Apparatus, Clearwater, FL). The short-circuit current (Isc) and transepithelial potential difference (PD) were measured using a voltage-current clamp (Physiological Instruments, San Diego, CA). Before tissue was mounted in the Ussing chamber, electrode polarization and fluid resistance was compensated with the VCC600 voltage-current clamp. Calomel electrodes (Fisher, Atlanta, GA) placed in a saturated KCl solution were connected to the Ussing chamber *via* salt bridges (4% agar in elasmobranch Ringer) to measure the PD. Platinum electrodes (Fisher, Atlanta, GA) were placed directly into the Ussing chamber to measure Isc. The PD and Isc were displayed on a Soltec 1242 strip chart recorder (Soltec Corp., Sun Valley, CA). Transepithelial resistance was calculated using the open-circuit PD, and the closed-circuit Isc of the mounted tissue. All readings were in reference to the luminal medium.

*Transport inhibitors*

Once baseline electrophysiological parameters were established, the percent change of Isc was calculated after the tissue was exposed to the following transport inhibitors: ouabain, $Na^+/K^+$ ATPase inhibitor ($10^{-4}$ *M*, serosal); bumetanide, $Na^+/K^+/Cl^-$ cotransport inhibitor ($10^{-3}$ *M*, se-

rosal); DIDS (4,4′-diisothiocyanatostilbene-2,2′-disulfonic acid, $Cl^-/HCO_3^-$ exchange inhibitor ($10^{-3}$ *M*, luminal); amiloride, sodium channel inhibitor, ($10^{-3}$ *M*, luminal and serosal); acetazolamide, carbonic anhydrase inhibitor ($10^{-5}$ *M*, luminal). Chloride was substituted in the medium with isomolar concentrations of gluconate. All reagents were purchased from Sigma Chemical Co., St. Louis, MO.

*Alkalinization rates*

The alkalinization rate of the luminal medium was measured using the pH stat technique on glands mounted in the Ussing chamber. Unbuffered (bicarbonate-free) Ringer bathing the luminal side of the gland was gassed with 100% oxygen during experiments and 30 min prior to tissue mounting. The serosal-bathing medium consisted of buffered elasmobranch Ringer, gassed with 95% oxygen/5% carbon dioxide. The rate of fluid alkalinization ($\mu$Eq of acid/cm$^2$/h) was then determined *via* titration using 0.01 *M* sulfuric acid. The pH of the luminal medium was maintained at pH 5.5 for at least six consecutive intervals of 5 min each. The pH was monitored using a pH microelectrode (Microelectrode, Londonderry, NH) connected to a Beckman pH meter (Omega 40, Fullerton, CA).

Two experiments were performed to determine the presence of either chloride-dependent or sodium-dependent bicarbonate transport. Alkalinization rates were measured after each manipulation. Baseline values were made from tissues bathed on both sides with elasmobranch Ringer. The medium was changed on the luminal and serosal sides to iso-osmotic elasmobranch Ringer free of chloride or sodium. In the first experiment, chloride-containing Ringer was added back to the luminal side; in the second experiment, sodium-containing Ringer was added back to the serosal side. After a new alkalinization rate was established, a bicarbonate transport inhibitor, SITS (4-acetamido-4′-isothiocyanatostilbene-2,2′-disulfonic acid, $10^{-3}$ *M*), was added to the luminal medium in both experiments.

The buffering capacity of the various Ringers was determined after each experiment, using the pH stat method. The buffering capacity of each medium was then subtracted from the alkalinization rate derived under the experimental conditions.

*Statistical analyses*

Statistical significance was evaluated using a two-tailed-paired *t* test, with the level of significance set at $P < 0.05$.

## Results

*Gross anatomy*

The alkaline gland of the Atlantic stingray, *Dasyatis sabina*, consists of a pair of blind-ended, bladder-like sacs located within the pelvic girdle ventral to the posterior pole of the kidney and lateral to the vas deferens. In the animals we examined, the glands were retroperitoneal and symmetrically aligned along the vertebral column. They were easily distinguished from surrounding tissue by their deep burgundy color. Each sac of the gland held a maximum of 4–5 ml of fluid. The mediocaudal portion of each gland narrowed to a single duct, which joined the respective sperm duct (vas deferens) on the same side of the animal. The resultant common duct for sperm and alkaline gland fluid was about 3-mm long and pierced the body wall to open on the crest of the urinary papilla in the cloaca.

*Microscopy*

The mucosa of the alkaline gland was highly folded and lined by a simple columnar epithelium (Figs. 1, 2). A rich capillary network lay immediately beneath the basement membrane. Within each fold were an arteriole and venule and dense tracts of nerve fibers (Figs. 1–3).

Two populations of epithelial cells were distinguished on the basis of their apical membrane exposure to the lumen (Fig. 1). The length of the long axis of the apical cell surface differed significantly in the two populations ($P < 0.05$, $n = 141$); in one (84.4% of the total cells) the long axis of the apical cell surface was $7.2 \pm 0.14$ $\mu$m; in the other (15.6%), the long axis was about twice that length ($14.92 \pm 0.49$ $\mu$m). All cells that contacted the lumen had the same ultrastructural organization, despite the difference in lumenal membrane area.

Columnar epithelial cells had a prominent, basally located pleomorphic nucleus and exceptionally large and abundant secondary lysosomes (Figs. 1, 2). The secondary lysosomes stained positively for lipofuscin (data not shown) and were dark green-brown in unstained sections. (Fig. 3). The smooth-surfaced endoplasmic reticulum was evenly distributed throughout the cytoplasm. Mitochondria bearing lamellar cristae were located in the upper two-thirds of the cell, and Golgi complexes were abundant in the perinuclear region (Fig. 2). Many membrane-bound vesicles were present in the Golgi region and adjacent to the apical plasma membrane. Some of these vesicles were seen fusing with larger vesicles as well as with the apical plasma membrane (Fig. 2).

Basal cells were also present in the lower third of the epithelium (Fig. 4) in a ratio of about 1 basal cell to 20 columnar cells. These cells, which ranged from 1.4 to 2.6 $\mu$m in diameter, were not highly interdigitated with adjacent columnar cells and were not observed in contact with another basal cell. The cytoplasm of basal cells surrounded a proportionately large nucleus and contained only a few organelles, which were limited to the endoplasmic reticulum, and small vesicles containing material of various degrees of electron density.

The apical surface of the columnar cells was elaborated

**Figure 1.**

**Figure 2.**

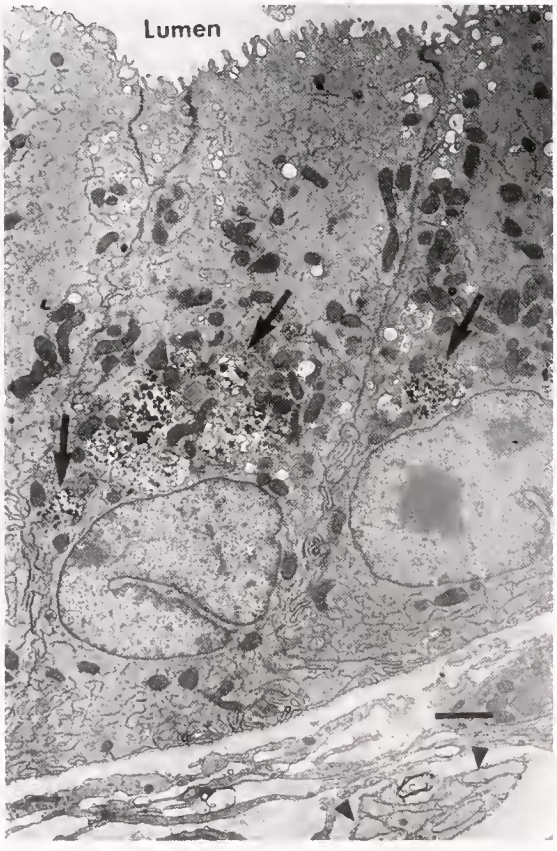


**Figure 3.**

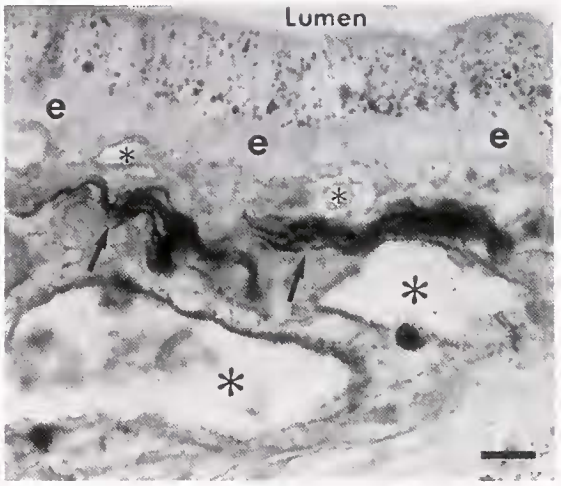


**Figure 4.**

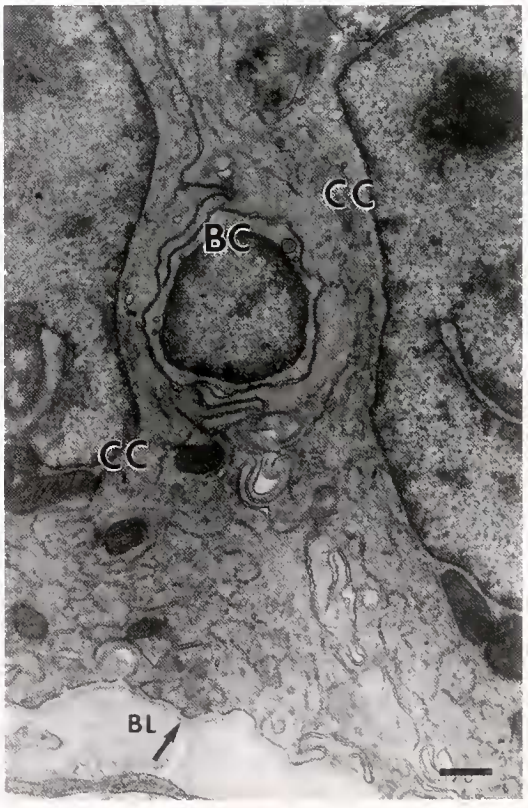

into microplicae (Figs. 1, 2). The basolateral plasma membrane was relatively straight nearest the lumen, but closer to the basal lamina it was interdigitated with itself and adjacent cells (Fig. 2). Freeze fracture of the lateral plasma membrane revealed some areas consisting only of large intramembranous particles (99 Å ± 0.1, $n = 52$) (Fig. 5) loosely arranged as single particles or in groups of up to 20 particles. Outside these areas was a mixture of large and small intramembranous particles. No rod-shaped particles were observed in either the apical or basolateral plasma membrane. The zonulae occludentes were deep (1.4 ± 0.7 μm, $n = 19$ replicas) and composed of 21.8(±4.5) fibrils (Fig. 6). Most of the fibrils were parallel to the apical plasma membrane, with those constituting the basal one-fourth of the zonulae occludentes forming a loose anastomosing network (Fig. 6).

Ultrastructural observations of the solids from alkaline gland fluid showed cellular debris including multivesicular bodies, spherical particles with electron-dense cores that stained positively for lipofuscin, membrane whorls, and a few necrotic spermatozoa (Fig. 7).

*Localization of carbonic anhydrase activity*

Carbonic anhydrase activity (CAH) was indicated by a black precipitate at both the light and electron microscopic level (Figs. 8, 9). A minimum of 2 min in the incubation medium was required for the precipitate to develop, at which time CAH appeared first within the intercellular space of columnar cells. In electron micrographs, CAH was localized in the intercellular space between columnar cells but excluded from the zonulae occludentes (Fig. 9). Adjacent to the basement membrane, CAH was observed only within the intercellular space formed by invaginations of the plasma membrane or interdigitation of cytoplasmic folds (Fig. 9). Regions of the basolateral plasma membrane that contacted the basement membrane did not exhibit CAH. After 3–10 min of incubation, the precipitate appeared in the basal two-thirds of columnar cell cytoplasm (Fig. 8).

Control sections incubated on bicarbonate-free Hansson's medium or on ammonium sulfide alone were similar to unstained sections that were rinsed only on Sorensen's phosphate buffer, and showed no positive staining (data not shown). Complete inhibition of CAH occurred at acetazolamide concentrations of $10^{-5}$ *M* in Hansson's medium (data not shown). Lower concentrations of acetazolamide ($10^{-6}$ *M*) failed to inhibit CAH activity for incubation periods longer than 2 min.

*Analysis of alkaline gland fluid (AGF)*

Table I shows the analyzed constituents of AGF. Sodium and chloride were the dominant ions, with $K^+$, $Mg^{++}$, $Ca^{++}$, and $Fe^{++}$ in detectable amounts. The osmolality was near that of plasma (750–875 mOsm), and significant concentrations of protein and urea were measured. The pH varied between 8.0 and 8.2.

*Electrophysiology*

*Baseline parameters.* The baseline PD was 14.5 ± 1.9 mV, Isc was 29.1 ± 4.2 μA/cm$^2$, and transepithelial resistance was calculated to be 732.4 ± 184.6 ohm · cm$^2$ ($n = 18$).

*Transport inhibitors.* The effect of specific ion transport inhibitors on the baseline Isc is shown in Table II. The serosal addition of ouabain, a $Na^+/K^+$ ATPase inhibitor, resulted in an almost 48% decrease of Isc within 45 to 50 min. Bumetanide, a $Na^+/K^+/Cl^-$ cotransport inhibitor, decreased the Isc approximately 70% within 30 min, and DIDS, a $Cl^-/HCO_3$-exchange inhibitor, placed on the luminal side of the epithelium decreased the Isc almost 38% within 30 to 40 min. The Isc was completely inhibited, and in fact was slightly reversed, after consecutive addition of bumetanide within 30 min of DIDS addition to the lumenal surface. The effect of luminal exposure to acetazolamide, a carbonic anhydrase inhibitor, on Isc was sporadic, and produced only a 16% overall reduction of Isc. Amiloride, a sodium ion channel inhibitor, placed in either the luminal or serosal media had no significant effect on the Isc (data not shown). The removal of chloride from the bathing media on both sides of the tissue with the substitution of gluconate resulted in a 67% reduction in Isc by 45 min.

*Alkalinization rates.* Two experiments investigating de-

**Figure 1.** Scanning electron micrograph of a transected mucosal fold. The asterisk is located in the center of an arteriole. A network of capillaries (arrows) lies directly beneath the epithelium, which has prominent secondary lysosomes (arrowheads). Bar = 50 μm.

**Figure 2.** Transmission electron micrograph (TEM) of the simple columnar epithelium of the alkaline gland. Arrows indicate secondary lysosomes located in the supranuclear region. Arrowheads indicate a nerve fiber closely adjacent to the epithelium. Note the numerous vesicles in the apical cytoplasm. Bar = 2 μm.

**Figure 3.** Light micrograph (LM) of nerve fibers (arrows) in the subepithelial lamina propria stained black using the Sevier Munger silver technique. Nerve fibers were closely associated with blood vessels (asterisks) and the epithelium (e). Note the multiple darkly staining secondary lysosomes in the apical cytoplasm of the epithelium. Bar = 4 μm.

**Figure 4.** TEM of a basal cell (BC) located between adjacent columnar cells (CC). Note the large proportion of the nucleus relative to the BC cytoplasm. Basal lamina (BL). Bar = 2 μm.

**Figure 5.**

**Figure 6.**

**Figure 7.**

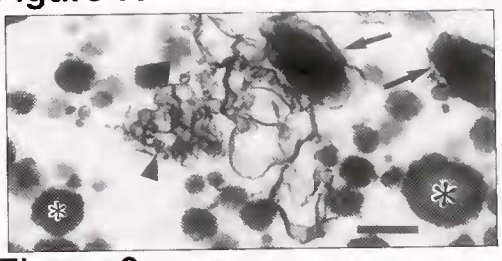

**Figure 8.**

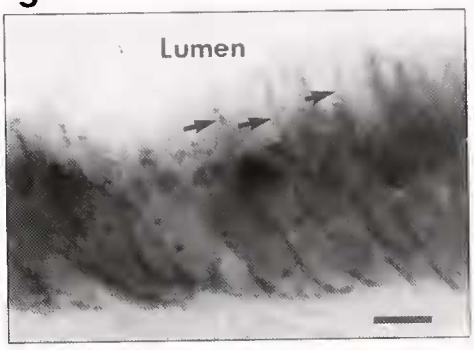


**Figure 9.**

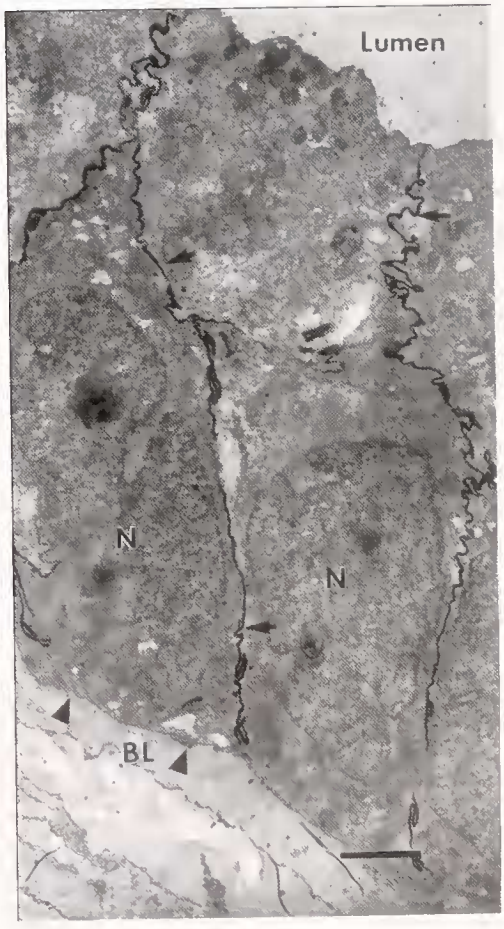

**Table I**

*Analyzed constituents of alkaline gland fluid*

| *Component* | *Concentration* |
|---|---|
| $Na^+$ | 286 m*M* |
| $K^+$ | 3.7 m*M* |
| $Cl^-$ | 113.0 m*M* |
| $Mg^{++}$ | 1.68 m*M* |
| $Ca^{++}$ | 0.84 m*M* |
| $Cu^{++}$ | 0.58 m*M* |
| $Zn^{++}$ | 0.87 m*M* |
| $Fe^{++}$ | 0.61 m*M* |
| Urea | 271 m*M* |
| Progesterone | 0.012 $\mu M$ |
| Estradiol | 0.16 p*M* |
| Norepinephrine | ND |
| Epinephrine | ND |
| Dopamine | ND |
| Testosterone | 4.3 $\mu M$ |
| Protein | 5.9 mg/ml |
| Osmolality | 875 mosm |

mosm = milliosmoles, ml = milliliter, mg = milligram, p*M* = picomoles, $\mu M$ = micromoles, m*M* = millimoles, ND = none detected.

**Table II**

*Effects of ion transport inhibitors on the short-circuit current (Isc)*

| Treatment | % Decrease of Isc | *n* |
|---|---|---|
| Ouabain ($10^{-4}$ *M*), S | 47.8 ± 2.9 | 4 |
| Bumetanide ($10^{-3}$ *M*), S | 69.7 ± 5.5 | 8 |
| DIDS ($10^{-3}$ *M*), L | 37.9 ± 5.9 | 6 |
| DIDS ($10^{-3}$ *M*), L + Bumetanide ($10^{-3}$ *M*), S | 105.9 ± 12.2 | 5 |
| Acetazolamide ($10^{-5}$ *M*), L | 16.0 ± 9.0 | 3 |

Values are means ± SE, L = Luminal, S = Serosal, *n* = number of mounted glands. DIDS = 4,4′-diisothiocyanatostilbene-2,2′-disulfonic acid.

pendent and independent bicarbonate transport mechanisms are shown in Table III. The baseline alkalinization rate of control tissues varied from about 4 to 7.5 $\mu$Eq of acid/cm$^2$/h depending upon the animal used.

Chloride-dependent bicarbonate secretion was demonstrated by a significant decrease in alkalinization rate when both sides of the gland were exposed to chloride-free Ringer (Table III, Experiment 1). Alkalinization returned to control levels when chloride was added back to the luminal side of the tissue. SITS ($10^{-3}$ *M*), a bicarbonate transport inhibitor, when applied to the luminal medium, had no statistically significant effect on the alkalinization rate after luminal exposure to chloride (Table III). However, the results varied widely from tissue to tissue.

In the second experiment, the fluid alkalinization rate decreased significantly, 55%, after luminal and serosal exposure to sodium-free media (Table III). The alkalinization rate increased immediately with the readdition of serosal sodium-containing Ringer. Addition of the bicarbonate transport inhibitor, SITS ($10^{-3}$ *M*), to the luminal medium caused a significant decrease (24%) in the alkalinization rate compared to the values after sodium readdition (Table III).

## Discussion

Results of this study extend the presence of alkaline glands in the Elasmobranchii to include stingrays. Our gross anatomical explorations of several species of shark—spiny dogfish, *Squalus acanthias;* black tip, *Carcharhinus limbatus;* smooth dogfish, *Mustelus canis;* scalloped hammerhead, *Sphyrna lewini,* and Atlantic sharpnose, *Rhizoprionodon terraenovae*—did not reveal the presence of alkaline glands in these elasmobranchs. This finding is consistent with the notion that alkaline glands are present only in skates and rays and not in sharks. Furthermore, this study is the first to elucidate the morphology, ion transport mechanisms, enzyme histochemistry, and fluid composition of the alkaline gland in a species of stingray.

The gross anatomy of the Atlantic stingray alkaline gland is similar to that described for several species of skates

**Figure 5.** Transmission electron micrograph (TEM) of freeze fracture replica of a loose cluster of large intramembranous particles (arrows) found on the P fracture face of the lateral plasma membrane. Bar = 270 nm.

**Figure 6.** TEM of freeze fracture replica of the zonula occludens between two columnar cells. Note that numerous strands are arranged in a parallel array near the gland lumen (asterisk), but the more basal strands form an anastomosing network (P fracture face). Bar = 200 nm.

**Figure 7.** TEM of solid constituents from centrifuged alkaline gland fluid. Arrows indicate degenerate sperm with outer plasma membrane separated from the sperm head. Arrowheads indicate masses of membranes. Asterisks show roughly globular particles that composed the greatest part of the alkaline gland particulate matter. Bar = 2 $\mu$m.

**Figure 8.** Light micrograph of carbonic anhydrase activity in epithelial cells lining the alkaline gland. Typical staining pattern in sections incubated for 3–10 min on Hansson's medium. Enzyme activity was strongly present in the intercellular spaces (arrows), as well as in the mid to basal cytoplasm of columnar cells. Bar = 7 $\mu$m.

**Figure 9.** TEM of carbonic anhydrase activity in sections incubated for 2 min on Hansson's medium. Enzyme activity appears as electron-dense precipitate (arrows) confined to the intercellular space. N = nuclei of columnar cells. Note the absence of CAH activity along the basal lamina (BL). Bar = 2 $\mu$m.

**Table III**

In vitro *alkalinization rates of alkaline glands*

| Experimental conditions | Alkalinization rate ($\mu$Eq of acid/cm$^2$/h) |
|---|---|
| *Experiment 1* | |
| Elasmobranch Ringer (Control) | 3.88 ± 0.63 |
| Chloride-free Ringer, L&S | −1.93 ± 1.89* |
| Chloride readdition, L | 3.65 ± 1.17** |
| Addition of SITS (1 m*M*), L | 1.45 ± 2.22 |
| *Experiment 2* | |
| Elasmobranch Ringer (Control) | 7.65 ± 0.67 |
| Sodium-free Ringer, L&S | 3.49 ± 0.41* |
| Sodium readdition, S | 5.64 ± 0.62** |
| Addition of SITS (1 m*M*), L | 4.30 ± 0.45*** |

Values are means ± SE; $n = 5$ for each experiment. L = luminal, S = serosal. SITS = 4-acetamido-4′-isothiocyanatostilbene-2,2′-disulfonic acid.

* Significant difference compared to control, ** significant difference compared to respective chloride or sodium free conditions, *** significant difference compared to respective chloride or sodium readdition, $P < 0.05$.

(Maren *et al.*, 1963). However, one significant difference is the relationship between the alkaline gland duct and the sperm duct. In skates, Maren *et al.* (1963) reported that the alkaline gland ducts and sperm ducts have separate openings onto the urinary papilla. In the stingray, the alkaline gland duct joins the sperm duct, and the resultant common duct then opens onto the urogenital papilla. This anatomical arrangement in the Atlantic stingray allows mixing of sperm and alkaline gland fluid (AGF), suggesting that AGF may facilitate successful fertilization by its actions on spermatozoa. Furthermore, the confluence of the two ducts in the Atlantic stingray may explain the presence of some necrotic sperm and cell membranes in AGF, because residual sperm in the common duct would have retrograde access to the alkaline gland lumen. The absence of spermatozoa in the AGF supports the contention that the gland is not a *bona fide* sperm storage organ, thus contradicting reports by early anatomists (Borcea, 1906; Daniel, 1934).

Morphological features of columnar cells composing the epithelium of the alkaline gland of the Atlantic stingray are generally consistent with preliminary reports of the alkaline gland of the little skate (Maren *et al.*, 1963; Masur, 1984). Those cells exhibited a well-developed Golgi apparatus and endoplasmic reticulum, suggesting a high degree of active protein synthesis. The many vesicles we observed in the cytoplasm, especially those budding from the Golgi apparatus and fusing with larger vesicles or with the apical plasma membrane, support that idea. Although basal cells were morphologically distinct from columnar cells, we are uncertain whether they are a separate population of mature cells or are immature columnar cells.

A striking microscopic feature of stingray alkaline gland epithelial cells was large secondary lysosomes that imparted a dark green-black color to the gland and were distinctive in unstained tissue sections. An accumulation of myelin figures and lipofuscin granules in these secondary lysosomes was strongly suggestive of increased lysosomal processing of lipid membrane (Reed *et al.*, 1965; Harman, 1990). Interestingly, such features were also observed in epithelial cells of mammalian male reproductive organs such as the epididymis and seminal vesicle (Pappenheimer and Victor, 1954; Nicander, 1958; Mitchinson *et al.*, 1975). Mitchinson *et al.* (1975) suggested that the spermatozoa in the lumen of those organs may be the source of the intracellular lipofuscin granules, whereby epithelial cells perform a "salvaging" function and store insoluble fatty acids as lipofuscin. A similar process may occur in alkaline gland epithelial cells: the necrotic sperm and cell debris observed in the lumen of the gland would be the extracellular source of the intracellular lipofuscin granules.

The composition of stingray AGF differs from that previously reported for three species of skates (Maren *et al.*, 1963) in several ways. Stingray AGF is a deep burgundy color and nearly opaque; in contrast, skate AGF is clear to slightly yellow. Stingray AGF has significant amounts of protein and urea; skate AGF is reported to lack protein and have only about one-third the concentration of urea found in the Atlantic stingray (Maren *et al.*, 1963). Furthermore, the ionic concentration was different: stingray AGF had one-half the concentration of $K^+$ and $Cl^-$ reported for skate AGF but 4 times more $Mg^{++}$ and $Ca^{++}$. The present study is the first to show AGF with immunodetectable steroid hormones. However, the immunological methods used antibodies to human hormones, which raises the possibility that the results may be due to nonspecific binding.

A recent study (Büllesbach *et al.*, 1997) probed the possibility that AGF contained relaxin, a peptide hormone found in mammalian reproductive tissues and secreted fluids. The fact that relaxin in mammalian seminal fluid stimulates sperm motility (Essig *et al.*, 1982; Weiss, 1989) was the basis for the investigation in the stingray. Büllesbach and colleagues (1997) showed that stingray AGF contains a unique relaxin-like molecule with an apparent molecular mass of 13 kDa formed by two polypeptide chains of 4 and 9 kDa. This molecule is the only member of the relaxin family known to be glycosylated. The relaxin-like molecule of stingray AGF did not alter stingray sperm motility *in vitro* (Büllesbach *et al.*, 1997), but this finding does not rule out the possibility that the AGF relaxin-like molecule acts on a different aspect of sperm function such as capacitation or that it functions in the female reproductive tract.

The lumen of the stingray alkaline gland was not lined by the villar projections described in the skate (Maren *et al.*, 1963), but it did have mucosal folds, each of which contained a major arteriole and venule. The apical plasma membrane of the columnar epithelial cells was elaborated into microvilli characteristic of a secreting epithelium.

Freeze fracture replicas showed that the only distinguishing intramembranous particles were in the basolateral plasma membrane. The size and distribution of the particles forming these clusters was comparable to those forming gap junctions in mammalian cells. Apical and basolateral plasma membranes did not reveal any rod-shaped particles that would suggest proton transport (Brown and Montesano, 1980).

The zonulae occludentes of columnar cells consisted of about 22 strands, suggesting that the epithelium is electrically tight and imparts a high transepithelial resistance (Claude and Goodenough, 1973; Claude, 1978). Our *in vitro* electrophysiological data showed that the transepithelial resistance was 732 ohm · $cm^2$, confirming the tight junction morphology. The presence of "very tight" zonulae occludentes and a high transepithelial resistance suggests that there is little paracellular solute transport across the epithelium of the alkaline gland (Bowman *et al.*, 1992; Byers and Marc-Pelletier, 1992). Therefore, regulation of ion transport appears to occur primarily across the plasma membrane.

Maren *et al.* (1963) and Smith (1981, 1985) have demonstrated that both bicarbonate and chloride are secreted in the little skate alkaline gland and that chloride is the main anion responsible for most of the Isc. This finding was extended to the stingray alkaline gland in the present study in which Isc decreased almost 70% when chloride was removed from the bathing medium. Using intracellular microelectrodes, Smith (1981, 1985) showed that the apical plasma membrane was dominated by a large chloride conductance, whereas the basolateral plasma membrane contained a barium-sensitive potassium channel. However, the mechanisms involved in the alkalinization process have never been clearly established in this gland, despite speculation that a $Cl^-/HCO_3^-$ exchanger may exist in the apical or basolateral plasma membrane or in both membranes (Maren *et al.*, 1963; Smith, 1981, 1985).

In the present study, the marked reduction in Isc after serosal addition of bumetanide, an inhibitor of $Na^+/K^+/Cl^-$ cotransport, suggests that this transporter is located in the basolateral plasma membrane. If so, it may be the main conductive pathway for chloride entry into the cell. The remaining Isc could be due to the secretion of intracellular chloride or another anion, such as bicarbonate. To test this latter possibility we added the stilbene, DIDS, which effectively inhibits bicarbonate cotransporters (Wiederholt *et al.*, 1985; Melvin and Turner, 1992) as well as chloride channels (Bretag, 1987) to the luminal side of the epithelium. The resultant 38% decrease of Isc, and its further reduction to nominal levels after the consecutive addition of serosal bumetanide, substantiates this assumption. Furthermore, complete reduction of the Isc by consecutive addition of DIDS and bumetanide suggests a pathway for chloride secretion across the epithelial cells *via* a $Na^+/K^+/Cl^-$ cotransporter at the basolateral plasma membrane, and a chloride channel at the apical plasma membrane.

Chloride movement across the epithelial basolateral plasma membrane, *via* a putative $Na^+/K^+/Cl^-$ cotransporter in epithelial cells in stingray alkaline gland, appears to be driven in part by $Na^+/K^+$ ATPase, as shown by the serosal addition of ouabain, which decreased the Isc by 48%. In contrast, ouabain completely abolished chloride secretion and Isc in the little skate alkaline gland (Smith, 1985).

The lack of significant alkalinization rates after the tissue was exposed to medium free of chloride and sodium suggests that there is little independent transport of bicarbonate. If a significant portion of the alkalinization process involves an apical $Cl^-/HCO_3^-$ exchanger—as our results suggest—the absence of luminal chloride could impede that process, resulting in the accumulation of intracellular bicarbonate. Such a scenario has been observed in the rat parotid acini: SITS, an inhibitor of bicarbonate transport, increased intracellular pH and was thought to stimulate bicarbonate secretion *via* anion channels (Pirani *et al.*, 1987; Melvin and Turner, 1992). Chloride channels in a number of different epithelia, including pancreatic duct, sweat gland duct, and respiratory epithelia, have been shown to transport bicarbonate (Gray *et al.*, 1989; Tabcharani *et al.*, 1989; Kunzelmann *et al.*, 1991) at a conductance as high as 50% of the conductance of chloride.

The remaining Isc may be accounted for by a $Na^+/HCO_3^-$ symport, as demonstrated in this study by using pH stat methodology. Such mechanisms for bicarbonate transport have been demonstrated in renal proximal tubule (Yoshitomi *et al.*, 1985), corneal endothelial cells (Wiederholt *et al.*, 1985), and gastric oxyntic cells (Curci *et al.*, 1987).

Alkalinization of the luminal medium in the present study was dependent on the presence of both apical chloride and serosal sodium. The changes attributed to the absence and readdition of sodium suggests the presence of a $Na^+/HCO_3^-$ symport. The alkalinization rate attributed to the readdition of serosal sodium, and its reduction by luminal SITS, is indirect evidence that a $Na^+/HCO_3^-$ symport may be located at the apical plasma membrane. The stilbene, SITS, blocks not only bicarbonate transport *via* $Na^+/HCO_3^-$ symporters (Curci *et al.*, 1987; Fitz *et al.*, 1989; Wiederholt *et al.*, 1985), but also $Cl^-/HCO_3^-$ exchangers (Stewart *et al.*, 1989).

Maren and co-workers (1963) demonstrated a possible relationship between CAH and higher pH levels in AGF of various skate species. They showed that inhibition of CAH *in vivo* reduced the pH of newly formed fluid to levels found in species that did not have glandular CAH. This was accomplished using intravenous injections of acetazolamide at least 10 times higher than the dose we used. In a study of rat distal colon, the need for high (millimolar) concentrations of acetazolamide to inhibit bicarbonate transport was

attributed to the drug's poor cellular penetration, the distribution of CAH within the cell, and the requirement of 99% inhibition of CAH for a significant decrease of Isc to occur (Feldman *et al.,* 1988). The effectiveness of acetazolamide in reducing the Isc of the stingray alkaline gland is questionable because of the erratic results from tissue to tissue. However, concentrations of acetazolamide greater than $10^{-4}$ *M* were not used in the present study, because reports have indicated that the drug interferes with other ion transport mechanisms (Nellens *et al.,* 1975; Weiner and Mudge, 1985). Because the response to acetazolamide in our experiments was not consistent, we conclude that, in the stingray alkaline gland, either higher concentrations of acetazolamide are required to reduce the Isc, or bicarbonate secretion is not completely dependent on the presence of CAH.

We chose Hansson's technique (Hansson, 1968) to localize CAH after indirect immunoperoxidase staining methods failed. Antibodies to mammalian carbonic anhydrase I and II failed to recognize stingray carbonic anhydrase, which has significant structural and kinetic differences from forms found in higher vertebrates (Maynard and Coleman, 1971; Maren, 1980b).

The presence of CAH in the intercellular space of epithelial cells has been demonstrated not only in the alkaline gland in the present study, but also in other tissues such as the gall bladder, duodenum, and sweat gland (Hansson, 1968), as well as in the teleost opercular epithelium (Lacy, 1983b) and the elasmobranch rectal gland (Lacy, 1983a). This subcellular site may indicate the presence of either a membrane-bound or soluble form of CAH (Maren, 1980a). The exclusion of CAH activity from portions of the plasma membrane that contact the basement membrane suggests that its function is important in areas of cell-cell contact. Another possibility is that a soluble form of CAH exists in the intercellular space. The mechanisms that would prevent its diffusion along the basal aspect of the cell are unknown. In any case, CAH in intercellular spaces suggests that a bicarbonate reservoir may exist between epithelial cells (Lacy, 1983a) or that membrane-bound CAH may transport carbon dioxide, protons, or bicarbonate into or out of the cell (Enns, 1967; Wistrand, 1984).

The exclusion of CAH from the apical region of the alkaline gland epithelial cells shown in the present study has been demonstrated in mitochondria-rich cells of the turtle bladder and interfoveolar epithelial cells of the rat stomach, both of which are thought to subserve bicarbonate secretion (Sugai and Ito, 1980; Fritsche *et al.,* 1991a). A pattern similar to that seen in the alkaline gland was displayed in microvillated cells and microplicated cells under conditions inhibiting acid secretion (Fritsche *et al.,* 1991b).

The difference in distribution pattern and stain development of CAH in the alkaline gland may reflect the presence of at least two carbonic anhydrase isozymes (Carter and Parsons, 1971). The appearance of CAH in the intercellular space after relatively short incubation periods may indicate a high-affinity membrane-bound carbonic anhydrase isozyme. A low-affinity cytoplasmic form of carbonic anhydrase in the stingray alkaline gland is suggested by the longer incubation periods necessary for intracellular stain development.

## Acknowledgments

This work was supported, in part, by the Slocum-Lunz Foundation (GMG), National Science Foundation (ERL # DCB 8903369), and the University Research Council, Medical University of South Carolina.

## Literature Cited

**Bancroft, J. D., and H. C. Cook. 1984.** Pigments. Pages 144–158 in *Manual of Histological Techniques.* Churchill Livingstone, New York.

**Borcea, I. 1906.** Recherches sur la systeme urogenital des Elasmobranches. *Arch. Zool. Exper. Gen.* **4(4):** 199–484.

**Bowman, P. D., M. du Bois, R. R. Shivers, and K. Dorovini-Zis. 1992.** Endothelial tight junctions. Pages 305–320 in *Tight Junctions,* M. Cereijido, ed. CRC Press, Ann Arbor, MI.

**Bretag, A. H. 1987.** Muscle chloride channels. *Physiol. Rev.* **67(2):** 618–724.

**Brown, D., and R. Montesano. 1980.** Membrane specialization in the rat epididymis. I. Rod-shaped intramembrane particles in the apical (mitochondria-rich) cell. *J. Cell Sci.* **45:** 187–198.

**Büllesbach, E. E., C. Schwabe, and E. R. Lacy. 1997.** Identification of a glycosylated relaxin-like molecule from the male Atlantic stingray, *Dasyatis sabina. Biochemistry* **36:** 10735–10741.

**Byers, S., and R. Marc-Pelletier. 1992.** Sertoli-sertoli cell tight junctions and blood-testis barrier. Pages 279–307 in *Tight Junctions,* M. Cereijido, ed. CRC Press, Ann Arbor, MI.

**Carter, M. J., and D. S. Parsons. 1971.** The isoenzymes of carbonic anhydrase: Tissue subcellular distribution and function significance, with particular reference to the intestinal tract. *J. Physiol.* **215:** 71–94.

**Claude, P. 1978.** Morphological factors influencing transepithelial permeability: A model for the resistance of the zonula occludens. *J. Membr. Biol.* **39:** 219–232.

**Claude, P., and D. A. Goodenough. 1973.** Fracture faces of zonulae occludente from "tight" and "leaky" epithelia. *J. Cell Biol.* **58:** 390–400.

**Curci, S., L. Debellis, and E. Fromter. 1987.** Evidence for rheogenic sodium bicarbonate cotransport in the basolateral membrane of oxyntic cells of frog gastric fundus. *Pflugers Arch.* **408:** 497–504.

**Daniel, F. J. 1934.** Urogenital system. Pages 300–303 in *The Elasmobranch Fishes,* F. J. Daniel, ed. University of California, Berkeley, CA.

**Enns, T. 1967.** Facilitation by carbonic anhydrase of carbon dioxide transport. *Science* **155:** 44–47.

**Essig, M., C. Schoenfeld, R. D-Eletto, R. Amelar, L. Dubin, B. G. Steinetz, M. O'Bryne, and G. Weiss. 1982.** Relaxin in human seminal plasma. *Ann. NY Acad. Sci.* **380:** 224–230.

**Feldman, G. M., S. F. Berman, and R. L. Stephenson. 1988.** Bicarbonate secretion in the distal colon *in vitro:* A measurement technique. *Am. J. Physiol.* **254:** C383–390.

**Fitz, J. G., M. Persico, and B. F. Scharschmidt. 1989.** Electrophysiological evidence for sodium-coupled bicarbonate transport in cultured rat hepatocytes. *Am. J. Physiol.* **256:** G491–500.

**Fritsche, C., J. G. Kleinman, J. L. W. Bain, R. R. Heinen, and D. A. Riley. 1991a.** Carbonic anhydrase in turtle bladder mitochondrial-rich luminal and subluminal cells. *Am. J. Physiol.* **260:** F431–442.

**Fritsche, C., J. G. Kleinman, J. L. W. Bain, R. R. Heinen, and D. A. Riley. 1991b.** Carbonic anhdrase and proton secretion in turtle bladder mitochondrial-rich cells. *Am. J. Physiol.* **260:** F443–458.

**Gray, M. A., A. Harris, L. Coleman, J. R. Greenwell, and B. E. Argent. 1989.** Two types of chloride channel on duct cells cultured from human fetal pancreas. *Am. J. Physiol.* **257:** C240–251.

**Hansson, H. P. J. 1967.** Histochemical demonstration of carbonic anhydrase activity. *Histochemie* **11:** 112–128.

**Hansson, H. P. J. 1968.** Histochemical demonstration of carbonic anhydrase activity in some epithelia noted for active transport. *Acta Physiol. Scand.* **73:** 427–434.

**Harman, D. 1990.** Lipofuscin and ceriod formation: The cellular recycling system. *Adv. Exper. Med. Biol.* **266:** 3–18.

**Ito, S., and M. J. Karnovsky. 1968.** Formaldehyde-glutaraldehyde fixatives containing trinitro compounds. *J. Cell Biol.* **39:** 168a.

**Kunzelmann, K., L. Gerlach, U. Frobe, and R. Greger. 1991.** Bicarbonate permeability of epithelial chloride channels. *Pfluger Arch.* **417:** 616–621.

**Lacy, E. R. 1983a.** Carbonic anhydrase localization in elasmobranch rectal gland. *J. Exp. Zool.* **226:** 163–169.

**Lacy, E. R. 1983b.** Histochemical and biochemical studies of carbonic anhydrase activity in the opercular epithelium of the euryhaline teleost, *Fundulus heteroclitus*. *Am. J. Anat.* **166:** 19–39.

**Maren, T. H., J. A. Rawls, J. W. Burger, and A. C. Myers. 1963.** The alkaline (Marshall's) gland of the skate. *Comp. Biochem. Physiol.* **10:** 1–16.

**Maren, T. H. 1980a.** Current status of membrane-bound carbonic anhydrase. *Ann. NY Acad. Sci.* **341:** 246–258.

**Maren, T. H. 1980b.** Kinetics, equilibrium and inhibition in the Hansson histochemical procedure for carbonic anhydrase: A validation of the method. *Histochem. J.* **12:** 183–190.

**Masur, S. K. 1984.** Electron microscopy of the alkaline gland epithelium of the little skate, *Raja erinacea*. *Bull. Mt. Desert Is. Biol. Lab.* **24:** 96–97.

**Maynard, J. R., and J. E. Culeman. 1971.** Elasmobranch carbonic anhydrase. Purification and properties of the enzyme from two species of shark. *J. Biol. Chem.* **246:** 4455–4464.

**Melvin, J. E., and R. J. Turner. 1992.** $Cl^-$ fluxes related to fluid secretion by the rat parotid: Involvement of $Cl^-/HCO_3^-$ exchanger. *Am. J. Physiol.* **262:** G393–398.

**Mitchinson, M. J., K. P. Sherman, and A. M. Stainer-Smith. 1975.** Brown patches in the epididymis. *J. Pathol.* **115:** 57–62.

**Nellens, H. N., R. A. Frizzell, and S. G. Schultz. 1975.** Effect of acetazolamide on sodium and chloride transport by *in vitro* rabbit ileum. *Am. J. Physiol.* **228:** 1808–1814.

**Nicander, L. 1958.** Studies on the regional histology and cytochemistry of the ductus epididymis in stallions, rams, and bulls. *ACTA Morph. Neerl. Scand.* **1:** 337.

**Pappenheimer, A. M., and J. Victor. 1954.** "Ceroid" pigment in human tissues. *Am. J. Pathol.* **22:** 395–413.

**Pirani, D., L. A. Evans, D. I. Cook, and J. A. Young. 1987.** Intracellular pH in the rat mandibular salivary gland: The role of Na-H and $Cl\text{-}HCO_3$ antiports in secretion. *Pflugers Arch.* **408:** 178–184.

**Reed, R., G. McMillan, S. Hartroft, and E. Porta. 1965.** Progress of medical science: Pathology and bacteriology. *Am. J. Med. Sci.* **250:** 116–137.

**Sevier, A. C., and B. L. Munger. 1965.** A silver method for paraffin sections of neural tissue. *J. Neuropathol. Exp. Neurol.* **24:** 130–135.

**Smith, H. W. 1929.** The composition of the body fluids of elasmobranchs. *J. Biol. Chem.* **81:** 407–419.

**Smith, P. L. 1981.** Electrolyte transport by the alkaline gland of the little skate, *Raja erinacea*. Mechanism of luminal alkalinization. *Bull. Mt. Desert Is. Biol. Lab.* **21:** 80–83.

**Smith, P. L. 1985.** Electrolyte transport by alkaline gland of little skate *Raja erinacea*. *Am. J. Physiol.* **248:** 346–352.

**Stewart, C. P., J. M. Winterhages, K. Heintze, and K. U. Petersen. 1989.** Electrogenic bicarbonate secretion by guinea pig gallbladder epithelium: Apical membrane exit. *Am. J. Physiol.* **256:** C736–749.

**Sugai, N., and S. Ito. 1980.** Carbonic anhydrase, ultrastructural localization in the mouse gastric mucosa and improvements in the technique. *J. Histochem. Cytochem.* **28(6):** 511–525.

**Tabcharani, J. A., T. J. Jensen, J. R. Riordan, and J. W. Hanrahan. 1989.** Bicarbonate permeability of the outward rectifying anion channel. *J. Membr. Biol.* **112:** 109–122.

**Weiner, I. M., and G. H. Mudge. 1985.** Pp. 887–907 in *The Pharmacological Basis of Therapeutics*. 7th Edition. MacMillan, New York.

**Weiderholt, M., T. J. Jentsch, and S. K. Kellar. 1985.** Electrogenic sodium-bicarbonate symport in cultured corneal endothelial cells. *Pfluger Arch.* **405 (Suppl. 1):** S167–171.

**Weiss, G. 1989.** Relaxin in the male. *Biol. Reprod.* **40:** 197–200.

**Wistrand, P. J. 1984.** Properties of membrane-bound carbonic anhydrase. *Ann. NY Acad. Sci.* **429:** 195–206.

**Yoshitomi, K., B-Ch. Burckhardt, and E. Fromter. 1985.** Rheogenic sodium-bicarbonate cotransport in the peritubular cell membrane of rat proximal tubule. *Pflugers Arch.* **405:** 360–366.